Article:
Santoro, A, Sambiagio, C, McGowan, PC et al. (1 more author) (2014) Synthesis and coordination chemistry of 1,1,1-tris-(pyrid-2-yl)ethane. Dalton Transactions, 44 (3). 1060 - 1069. ISSN 1477-9226

https://doi.org/10.1039/c4dt02824d

Synthesis and Coordination Chemistry of 1,1,1-*Tris*-(pyrid-2-yl)ethane†

Amedeo Santoro,* Carlo Sambiagio, Patrick C. McGowan and Malcolm A. Halcrow*

A new synthesis of 1,1,1-*tris*(pyrid-2-yl)ethane (*L*), and a survey of its coordination chemistry, are reported. The complexes $[ML_2]^{n+}$ (M^{n+} = Fe^{2+}, Co^{2+}, Co^{3+}, Cu^{2+} and Ag^{+}), $[PdCl_2L]$ and [CuI(*L*)] have all been crystallographically characterised Noteworthy results include an unusual square planar silver(I) complex $[Ag(L)_2]X$ (X^- = NO_3^- and SbF_6^-); the oxidative fixation of aerobic CO_2 by [CuI(*L*)] to yield $[Cu_2I(L)_2(\mu\text{-}CO_3)]_2[CuI_3]$ and $[Cu(CO_3)(L)]$; and, water/carbonato tape and water/iodo layer hydrogen bonding networks in hydrate crystals of two of the copper(II) complexes. Cyclic voltammetric data on $[Fe(L)_2]^{2+}$ and $[Co(L)_2]^{2+/3+}$ imply that the peripheral methyl substituent has a weak influence on the ligand field exerted by *L* onto a coordinated metal ion.

Introduction

Tris-(pyrid-2-yl)methane, *tris*-(pyrid-2-yl)amine, *tris*-(pyrid-2-yl)phosphine and related compounds were first synthesised in the first half of the 20th century,[1] and developed as tripodal ligands for transition ions in the 1960-1980s.[2-4] Despite this long-standing chemistry, they continue to find use as facial protecting groups in organometallic chemistry,[5-7] catalysis,[8] transition metal photochemistry,[9] molecular magnetism[10-14] and other aspects of coordination chemistry.[15] A number of such ligands py_3X (py = 2-pyridyl) have been prepared, with different bridgehead groups 'X' (Scheme 1).

During our continuing research into the coordination chemistry of polydentate heterocyclic ligands,[16] we have fortuitously found a convenient synthesis of 1,1,1-*tris*-(pyrid-2-yl)ethane (*L*, Scheme 1). The synthesis of *L* by a different route has only been recently reported, and its coordination chemistry has been little explored.[7] We report here a survey of complexes of this ligand, and a comparison with other complexes from this family.

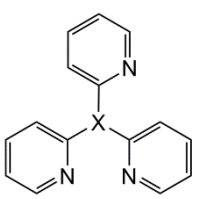

X = CH, CNH_2, COH, COMe, Cpy
N, P, P=O, As
BR^-, AlR^-
SiR, SnR, GeR
Sn^-, Pb^-

X = CMe (*L*)

Scheme 1 Examples of tripodal *tris*-pyridyl ligands that have been used in coordination and organometallic chemistry (py = 2-pyridyl).

Results and Discussion

Ligand *L* has been previously prepared by alkylation of deprotonated, pre-formed *tris*-(pyrid-2-yl)methane with MeI.[7] We have obtained it through an alternative one-pot procedure, by treatment of monolithiated 2-ethylpyridine with 2 equiv of 2-fluoropyridine.[17] This procedure afforded microanalytically pure ligand *L* in 78% yield following the usual work-up, without further purification. The addition of two pyridyl groups to 2-ethylpyridine, despite the presence of only one equiv of base in the reaction mixture, was unexpected but may reflect deprotonation of the acidic intermediate Py_2CHMe by the excess 2-fluoropyridine reagent, or by liberated F^-.[18] The identity of *L* was also confirmed crystallographically (ESI†).

The synthesis of $[ML_2][ClO_4]_2$ (M = Fe, **1**; M = Co, **2**) was performed by reaction of 2 equiv of *L* with the appropriate hydrated $M[ClO_4]_2$ salt, in MeCN under an N_2 atmosphere. Performing the cobalt synthesis in air afforded instead the cobalt(III) complex product $[CoL_2][ClO_4]_3$ (**3**) in good yield. The *tetrakis*-acetonitrile solvates of all three complex salts, and a second monohydrate form of **3**, were all crystallographically characterised (Fig. 1, Table 1 and ESI†). The complex molecules in all four structures have the expected six-coordinate geometry, with crystallographically imposed inversion symmetry. The metric parameters in all the complexes are consistent with low-spin iron(II), cobalt(II) and cobalt(III) centres (Table 1 and ESI†). Unusually, a crystallographically ordered Jahn-Teller elongation is evident in the $[CoL_2]^{2+}$ molecule in **2**. Low-spin cobalt(II) complexes of Py_3X and other *N*-heterocyclic chelates often exhibit dynamic

disorder of the Jahn-Teller distortion around the different N−Co−N axes (see below), which is only frozen out at very low temperatures.[13,19] The Fe−N and Co−N distances in **1**-**3** are similar to other published compounds of the $[M(Py_3X)_2]^{n+}$ type (M = Fe(II),[13,14,20,21] Co(II)[12,13,22] or Co(III)[12,23]; Scheme 1), showing that the *L* methyl substituent has little steric influence on the stereochemistry of the bound ligand.

Table 1 Selected bond distances and angles in the crystal structures of the iron and cobalt complexes (Å, º). See Fig. 1 and the ESI† for the atom numbering scheme employed, and for data from the hydrate crystal **3**·H_2O.[a]

	1·4MeCN M = Fe	**2**·4MeCN M = Co	**3**·4MeCN M = Co
M(1)–N(1)	1.971(2)	1.975(2)	1.9519(13)
M(1)–N(2)	1.972(2)	1.973(2)	1.9484(13)
M(1)–N(3)	1.976(2)	2.155(2)	1.9452(13)
N(1)–M(1)–N(1^i)	180	180	180
N(1)–M(1)–N(2)	88.34(9)	87.20(9)	88.90(5)
N(1)–M(1)–N(2^i)	91.66(9)	92.80(9)	91.10(5)
N(1)–M(1)–N(3)	88.12(9)	86.80(9)	88.87(5)
N(1)–M(1)–N(3^i)	91.88(9)	93.20(9)	91.13(5)
N(2)–M(1)–N(2^i)	180	180	180
N(2)–M(1)–N(3)	88.20(9)	86.84(9)	88.62(5)
N(2)–M(1)–N(3^i)	91.80(9)	93.16(9)	91.38(5)
N(3)–M(1)–N(3^i)	180	180	180

[a]Symmetry code: (i) *–x*, 1*–y*, 1*–z*.

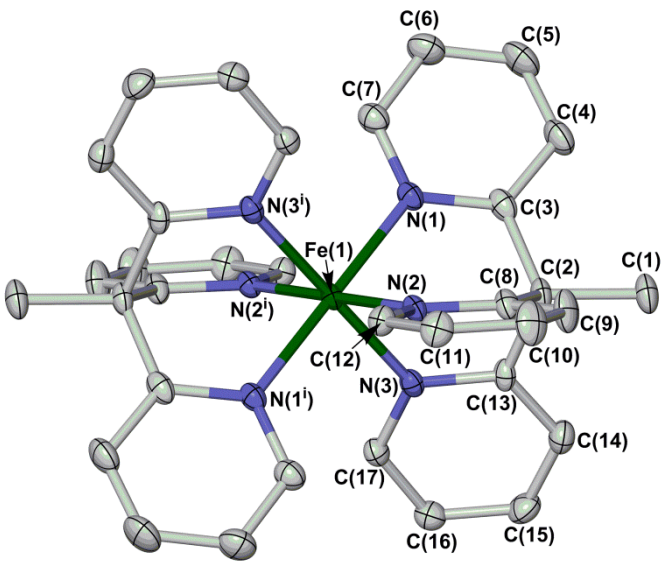

Fig. 1. View of the $[FeL_2]^{2+}$ cation in the crystal structure of **1**·4MeCN. Displacement ellipsoids are drawn at the 50 % probability level, and H atoms have been omitted for clarity. Symmetry code (i) *–x*, 1*–y*, 1*–z*. Colour code: C, white; Fe, green; N, blue. The same atom numbering scheme is also used for the solvate crystal structures of **2** and **3**, with Fe(1) replaced by Co(1) (ESI†).

Room temperature magnetic susceptibility and NMR data from **1** and **3** show they are diamagnetic and hence low-spin, which is in line with precedent. Variable temperature magnetic susceptibility data from **2** indicate that the material is low-spin below 200 K ($\chi_M T$ = 0.4 $cm^3mol^{-1}K$), but exhibits the onset of a gradual thermal spin-equilibrium on further warming (Fig. 2).

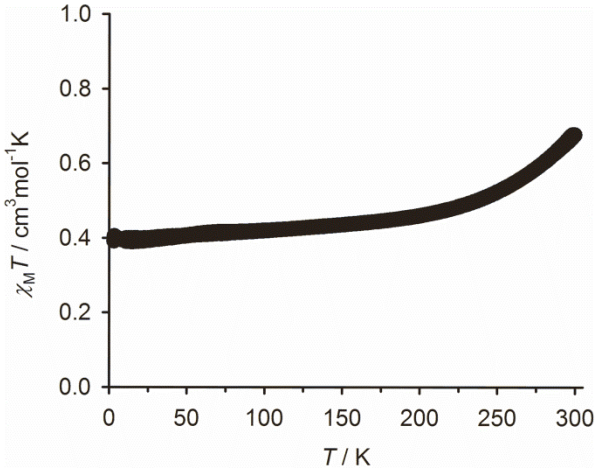

Fig. 2. Variable temperature magnetic susceptibility data from a dried powder sample of **2**.

The midpoint temperature of this spin-crossover ($T_{½}$) is estimated as >400 K. Comparable, gradual spin-crossover equilibria are shown by some salts of other $[Co(Py_3X)_2]^{2+}$ complexes (X = N,[11] CPy;[13] Scheme 1).

Cyclic voltammograms of **1** and **2** in MeCN/0.1 M NBu_4ClO_4 exhibit chemically reversible M(II/III) oxidations at $E_{½}$ = +0.61 V (**1**, M = Fe) and −0.31 V (**2**, M = Co) *vs.* Fc/Fc^+ (ESI†). These half-potentials are both *ca.* 0.1 V more negative than those reported for $[M(Py_3CH)_2]^{2+}$ (M = Fe[20,23] and Co[3,24]), bearing in mind the different reference electrodes used in literature studies. Given the lack of any steric influence of the *L* methyl group on the coordination spheres of **1**-**3** in the crystal, this cathodic shift probably reflects the electron donating properties of the *L* methyl substituent. A chemically reversible Co(II/I) couple is also shown by **2** at $E_{½}$ = −1.54 V, which is similar to that in $[Co(Py_3CH)_2]^{2+}$.[24]

Treatment of $[PdCl_2(NCMe)_2]$ with 1 equiv *L* in MeCN affords $[PdCl_2L]$ (**4**) as a yellow solid. This is a typical square planar palladium(II) complex by X-ray crystallography, containing a bidentate *L* ligand with one uncoordinated pyridyl group (ESI†). Complexation of $AgNO_3$ or $AgSbF_6$ by either 1 or 2 equiv *L* under the same conditions affords the salts $[AgL_2]Y$ ($Y^- = NO_3^-$, **5a**; $Y^- = SbF_6^-$, **5b**). While the nitrate salt **5a** afforded X-ray quality single crystals, the more soluble **5b** was used for solution measurements. The single crystal structure of **5a** reveals an unusual square planar silver(I) centre (Fig. 3, Table 2),[25,26] which is stereochemically comparable to the literature compound $[Pd(Py_3CH)_2][NO_3]_2$.[27] While the bond angles about the silver ion show only small deviations from the idealised D_{2d} symmetry imposed by this ligand geometry, the Ag−N distances show more variation. The bonds to one *L* ligand are strongly inequivalent, with Ag(1)–N(1) being 0.207(2) Å shorter than Ag(1)–N(2). In contrast the other ligand is bound more symmetrically, with Ag(1)–N(4) being 0.041(2) Å shorter than Ag(1)–N(5) (Table 2). The axial silver coordination sites are sterically shielded by the two pendant pyridyl groups. However the closest Ag...C distances to these

Table 2 Selected bond distances and angles in the crystal structure of **5a** (Å, °). See Fig. 3 and the ESI† for the atom numbering scheme employed.

Ag(1)–N(1)	2.2857(17)	Ag(1)–N(4)	2.3716(18)
Ag(1)–N(2)	2.4930(17)	Ag(1)–N(5)	2.3309(17)
N(1)–Ag(1)–N(2)	79.52(6)	N(2)–Ag(1)–N(4)	168.63(6)
N(1)–Ag(1)–N(4)	111.29(6)	N(2)–Ag(1)–N(5)	88.65(6)
N(1)–Ag(1)–N(5)	168.12(6)	N(4)–Ag(1)–N(5)	80.58(6)

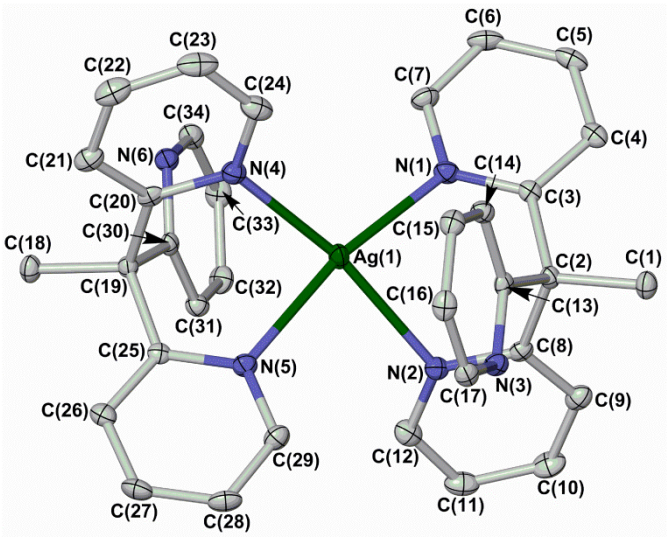

Fig. 3. View of the $[AgL_2]^{2+}$ cation in the crystal structure of **5a**. Displacement ellipsoids are drawn at the 50 % probability level, and H atoms have been omitted for clarity. Colour code: C, white; H, pale grey; Ag, green; N, blue.

groups are Ag(1)...C(13) = 2.9478(18) and Ag(1)...C(30) = 2.9430(18) Å, which are too long to be considered Ag... π contacts.[28] The nitrate ion does not interact with the silver centres and occupies a hydrophobic pocket in the lattice (the closest Ag...O distance is 5.3942(16) Å). The assignment of **5a** as a silver(I) complex, despite its unexpected coordination geometry, was supported by a bond valence sum (BVS) analysis which yielded an oxidation state of +1.00 for the silver ion.[29] Notably, square planar silver(I) complexes have also been obtained with other *tris*-heterocyclic ligands related to *L*.[26,30]

The room-temperature ^{1}H NMR spectrum of **5b** in $(CD_3)_2CO$ shows four aromatic peaks of equal integral arising from just one pyridyl environment, which is inconsistent with the crystal structure of **5a**. The chemical shifts of these resonances vary substantially on cooling, and begin to broaden at 263 K. At 183 K, although the spectrum was still broadened, the peaks had clearly decoalesced into two groups of aromatic resonances with an approximate 2:1 integral ratio (Fig. 4). That implies the $[AgL_2]^+$ complex retains a square planar geometry in solution, with the coordinated and uncoordinated pyridyl groups being in rapid chemical exchange. This fluxionality is more rapid than in the analogous square-planar palladium complex $[Pd(Py_3CH)_2][NO_3]_2$, whose coordinated and uncoordinated pyridyl rings are resolved by ^{1}H NMR at room temperature.[27]

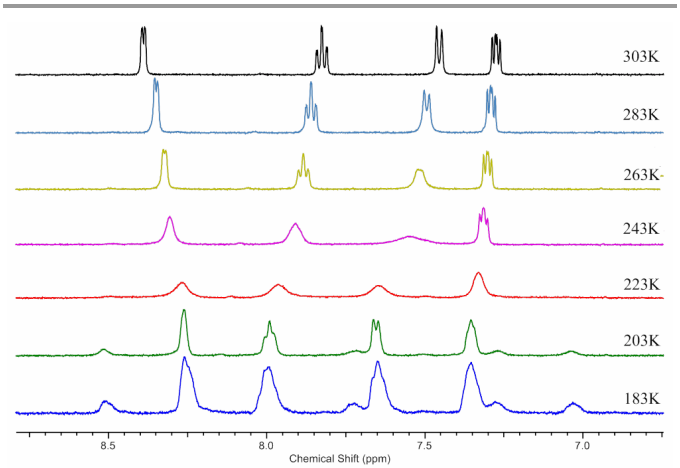

Fig. 4. Variable temperature ^{1}H NMR spectra of **5b** in $(CD_3)_2CO$.

Since Py_3X ligands have proven useful for stabilising unusual oxidation states of transition ions,[12] and d^9 silver(II) centres favour tetragonal coordination geometries,[31] the cyclic voltammogram of **5b** in MeCN/0.1 M NBu_4BF_4 was investigated. An oxidation at $E_{½}$ = +1.71 V *vs.* Fc/Fc$^+$ was observed, and assigned to an Ag(I/II) couple. This process was partly reversible at 298 K at a scan rate of 500 mVs^{-1} and its chemical reversibility diminished at lower scan rates, becoming essentially irreversible at 50 mVs^{-1}. Because of its low stability and positive potential, the chemical characterisation of $[AgL_2]^{2+}$ was not pursued further.

Complexation of CuI by 1 equiv *L* in MeCN afforded [CuI(*L*)] (**6**), which has a distorted tetrahedral geometry by X-ray crystallography (ESI†). Although air-stable in the solid state and in solution under an inert atmosphere, **6** undergoes a series of colour changes in acetonitrile upon exposure to air. Three products were isolated from these solutions under different conditions. Green, dinuclear $[Cu_2L_2I(\mu\text{-}CO_3)]_2[CuI_3]\cdot 2H_2O$ (**7a**) precipitates from aerobic acetonitrile solutions of **6**. This was crystallised from dmf/Et_2O as a solvate of $[Cu_2L_2\{I_m(OH)_{1-m}\}(\mu\text{-}CO_3)]_2[CuI_3]$ (**7b**; $m \approx 0.5$), in which the terminal iodo ligand has been partially substituted by exogenous hydroxide. Solutions of **6** or **7a** in water/acetonitrile mixtures crystallise more slowly, affording blue $[Cu(CO_3)L]\cdot 4.25H_2O$ (**8**) and $[CuL_2]I_2\cdot 8H_2O$ (**9**). While **9** was isolated in pure form, **8** was always contaminated by **9** which prevented a successful microanalysis from being obtained. Hence only the crystal structure of **8** is reported here.

Compounds **7a** and **8** arise from the fixation of atmospheric CO_2 by an aerobically oxidised $[CuL]^{2+}$ fragment.[32] Consistent with that, no reaction was observed when **6** was incubated with dry or wet CO_2 under an inert atmosphere, showing that aerobic oxidation to copper(II) is an essential first step of the transformation. A comparable reaction of the $[Cu(Py_3N)]^{+/2+}$ system under an atmosphere of CO_2 has been previously reported.[33] A dinuclear $[\{Cu(Py_3N)\}_2(\mu\text{-}CO_3)]^{2+}$ product was proposed in that study, but not crystallographically characterised; other $[Cu_2(\mu\text{-}CO_3)]^{2+}$ complexes are well known,

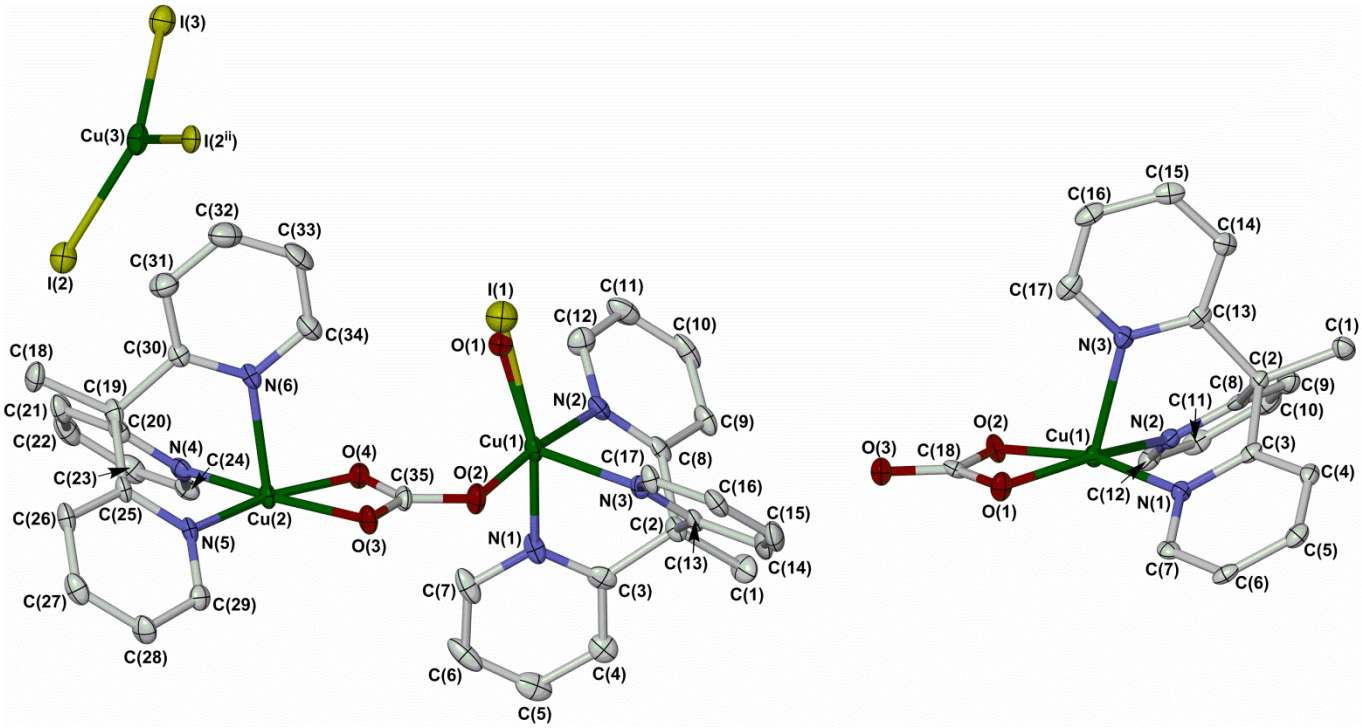

Fig. 5. Left: view of the $[Cu_2L_2\{I_m(OH)_{1-m}\}(\mu\text{-}CO_3)]^+$ cation and the $[CuI_3]^{2-}$ anion in the crystal structure of **7b**·4dmf·0.4H_2O. Right: one of the four unique complex molecules in the crystal structure of **8**·4.25H_2O. Displacement ellipsoids are drawn at the 50 % probability level, and H atoms have been omitted for clarity. Symmetry code (ii) 2–*x*, *y*, $^3/_2$–*z*. Colour code: C, white; Cu, green; I, yellow; N, blue; O, red.

however, with a variety of carbonate coordination modes.[33-35] No crystallographically authenticated mononuclear Cu/CO_3 complex with a tridentate co-ligand has been reported before.

The complex cation in **7b** contains two five-coordinate $[CuL]^{2+}$ centres (Fig. 5). Atom Cu(1) is also ligated by monodentate coordination of the bridging carbonate ligand and a mono-atomic donor that was refined as a mixture of iodide and an oxygen donor, which should be a hydroxo group on charge neutrality grounds. The Cu(1)–I(1) [2.5102(17) Å] and Cu(1)–O(1) [2.031(10) Å] distances are consistent with that interpretation. In contrast, the coordination sphere of Cu(2) is completed by bidentate coordination of the carbonato ligand. This $\kappa^1{:}\kappa^2,\mu\text{-}CO_3^{2-}$ coordination mode has been observed in several complexes of copper(II)[33,35,36] and other transition ions.[37] Both copper ions have near-ideal square-pyramidal geometries according to their τ parameters [0.172(4)/0.217(6) for Cu(1), calculated from I(1) and O(1) respectively, and 0.019(4) for Cu(2)].[38] The $[CuI_3]^{2-}$ counterion in **7b** has crystallographically imposed C_2 symmetry, and shows only small deviations from a triangular geometry.

The asymmetric unit of **8**·4.25H_2O contains four formula units of the compound (Z' = 4); that is, four independent molecules of the complex and seventeen water molecules. The connectivity of the complex is the same as for Cu(2) in **7b** (Fig. 5), but the unique molecules differ in their coordination geometry with τ ranging from 0.001(3) to 0.275(3).[38] The water molecules are crystallographically ordered and occupy channels in the lattice running parallel to the [100] vector. The channels are roughly rectangular in shape, and have the approximate dimensions 2.8 x 5.0 Å. The network has a complicated tape topology,[39] composed of fused four-, five- and six-membered rings of water molecules; and, four-, five-, six-, seven- and eight-membered hydrogen-bonded rings containing one or two carbonato groups (Fig. 6).

The $[CuL_2]^{2+}$ dication in **9**·8H_2O has a typical six-coordinate geometry, comparable to $[ML_2]^{n+}$ (M = Fe, Co) in **1**-**3** (Fig. 1). The cation has crystallographic 2/*m* symmetry, with an apparently compressed Jahn-Teller distortion along the unique N–Cu–N axis. However, a mean square displacement amplitude (MSDA) analysis[40] of the metal coordination sphere implies that this is a crystallographic artifact. Rather, the complex probably exhibits symmetry-imposed disorder of a more typical Jahn-Teller elongation along the other two, crystallographically equivalent N–Cu–N directions (ESI†).[41] Such Jahn-Teller disorder is a well-known phenomenon in copper(II) complexes,[42] including $[Cu(Py_3CH)_2][NO_3]_2$ and a hydrate of $[Cu(Py_3P)_2]Br_2$.[43] The hydrogen bond network in **9**·8H_2O is complicated by symmetry-imposed disorder of the water H atoms, but forms 2D sheets in the (001) plane with an L4(6)5(6)8(10) topology[39] comprised of $[(H_2O)_4]$, $[I(H_2O)_4]$ and $[I_2(H_2O)_6]$ rings (Fig. 7 and ESI†).

Conclusions

A new synthesis of *L* has been achieved, which may be a useful new facial protecting group for coordination and

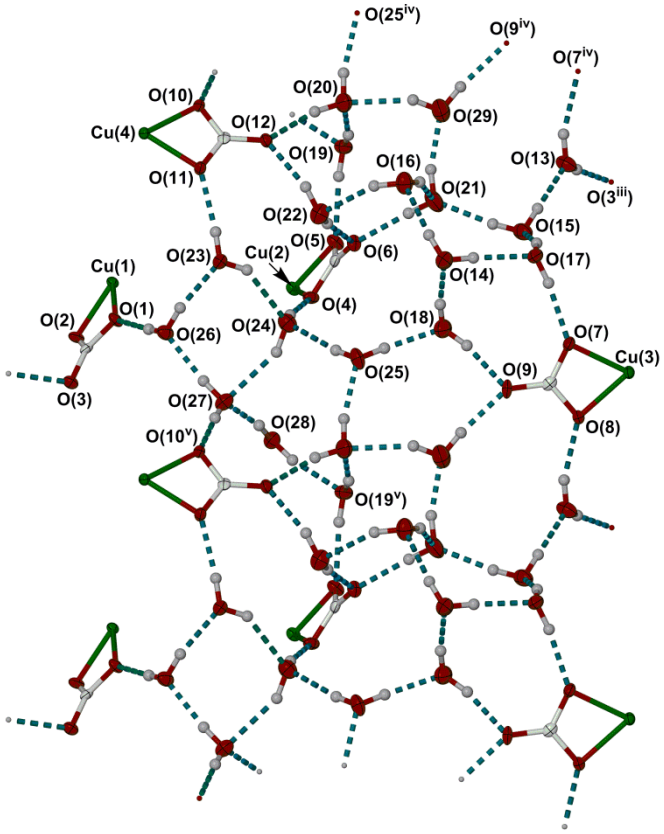

Fig. 6. View of the network of water molecules and carbonato ligands in **8**·4.25H_2O. The crystallographic *a* axis is vertical. Metric parameters for these hydrogen bonds are in the ESI†. Symmetry codes: (iii) 1–*x*, ½+*y*, 2–*z*; (iv) –1+*x*, *y*, *z*; (v) 1+*x*, *y*, *z*. Colour code: C, white; H, pale grey; Cu, green; N, blue; O, red.

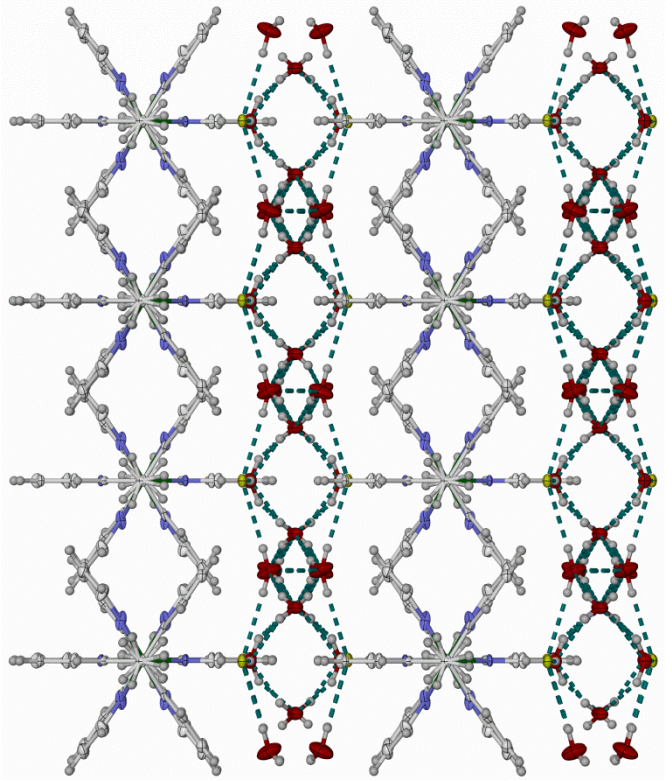

Fig. 7. Packing diagram of 9·8H_2O, showing the sheets of iodide ions and water molecules between the layers of cations. The view is parallel to the [100] crystal vector, with *b* vertical. A detailed view of the hydrogen bond network is in the ESI†. Colour code: C, white; H, pale grey; Cu, green; I, yellow; N, blue; O, red.

organometallic chemistry. The methyl substitutent protects the bridgehead C atom in *L* from external attack more effectively than the C–H group in *tris*-(pyrid-2-yl)methane, which is somewhat acidic,[7] but has only a small influence on the coordinating properties of *L*. While surveying the coordination chemistry of *L* we have obtained an unusual square planar silver complex $[AgL_2]^+$; observed two complicated and attractive water networks in hydrated crystals; and shed further insight into a previously reported CO_2 fixation reaction.[31] The dinuclear nature of the initial product of the transformation, **7a**, has been confirmed crystallographically. However, we have also now shown that aqueous solutions of **7a** react further, forming mononuclear copper/carbonato (**8**) and ligand disproportionation products (**9**).

Experimental

The precursor $[PdCl_2(NCMe)_2]$ was prepared by the literature procedure.[44] Unless otherwise stated, all other reagents and solvents were used as commercially supplied without further purification. **CAUTION** *Although we have experienced no problems with the perchlorate salt products in this work, metal-organic perchlorates are potentially explosive and should be handled with due care in small quantities.*

Synthesis of *tris*-(2-pyridyl)methylmethane (*L*). 2-Ethylpyridine (2.13 cm^3, 18.7 mmol) was dissolved in dry THF (60 cm^3) and cooled to −78°C in a dry ice-acetone bath. *n*-Buthylithium (7.5 cm^3 of a 2.5M solution in hexanes) was added dropwise, and the mixture was left to stir for 15 min. 2-Fluoropyridine (3.6 g, 37.4 mmol) was added slowly, keeping the reaction temperature below −30°C. After the addition was complete, the mixture was warmed to room temperature, then heated to reflux for 12 h. After cooling to room temperature, the reaction was quenched with excess water. The resultant off-white precipitate was collected, air-dried, then re-suspended in hexane and stirred for 2h. The solid was re-collected by filtration, affording *L* as an analytically pure off-white solid. Yield 3.8 g, 78 %. Found C, 77.9; H, 5.80; N, 16.1 %. Calcd for $C_{17}H_{15}N_3$ C, 78.1; H, 5.79; N, 16.1 %. ES MS *m/z* 262.13 ($[LH]^+$), 545.24 ($[Na(L)_2]^+$). ^{1}H NMR ($\{CD_3\}_2SO$) δ 2.20 (s, 3H, CCH_3), 7.02 (d, 8.1 Hz, 3H, Py H^3), 7.21 (ddd, 1.1, 4.8 and 7.5 Hz, 3H, Py H^5); 7.67 (pseudo-dt, 1.9 and 7.7 Hz, 3H, Py H^4), 8.50 (m, 3H, Py H^6). ^{13}C NMR ($\{CD_3\}_2SO$) δ 27.1 (1C, CCH_3), 56.9 (1C, CCH_3), 121.3 (3C, Py C^3), 123.3 (3C, Py C^5), 136.0 (3C, Py C^4), 148.3 (3C, Py C^6), 165.5 (3C, Py C^2).

Synthesis of $[FeL_2][ClO_4]_2$ (1). A solution of *L* (500 mg, 1.90 mmol) and $Fe[ClO_4]_2·6H_2O$ (242 mg, 0.95 mmol) in acetonitrile (15 cm^3) was stirred at room temperature under N_2 until all the solid had

dissolved. Addition of excess water precipitated the product, which was collected by filtration. The red-brown complex was recrystallised from an acetonitrile-water mixture. Yield 453 mg, 61 %. Found C, 52.5, H, 3.85; N, 10.7; Cl, 9.3 %. Calcd for $C_{34}H_{30}Cl_2FeN_{10}O_8$ C, 52.5; H, 3.89; N, 10.8; Cl, 9.1 %. ES MS *m/z* 289.09 ($[FeL_2]^{2+}$). ^{1}H NMR (CD_3NO_2) δ 3.07 (s, 6H, CH_3), 7.17 (pseudo-t, 6.3 Hz, 6H, Py H^5), 7.47 (dd, 1.3 and 6.9 Hz, 6H, Py H^3), 8.07 (pseudo-dt, 1.7 and 8.2 Hz, 6H, Py H^4), 8.21 (d, 5.9 Hz, 6H, Py H^6). ^{13}C NMR (CD_3NO_2) δ 21.4 (2C, CCH_3), 55.0 (2C, CCH$_3$), 121.9 and 124.8 (both 6C, Py C^3 and C^5), 138.5 (6C, Py C^4), 158.1 (6C, Py C^6), 163.6 (6C, Py C^2).

Synthesis of [CoL_2][ClO$_4$]$_2$ (2). Co[ClO$_4$]$_2$·6H$_2$O (104 mg, 0.29 mmol) and *L* (150 mg, 0.57 mmol) were dissolved in dry acetonitrile was dissolved in dry acetonitrile (15 cm^3), and stirred under N_2 until all the solid had dissolved. The solution was concentrated and filtered. Slow diffusion of diethyl ether vapour into this solution afforded orange crystals of the product. Yield 159 mg, 71 %. Found C, 51.7; H, 3.80; N, 10.5; Cl, 8.8 %. Calcd for $C_{34}H_{30}Cl_2CoN_{10}O_8$ C, 52.3; H, 3.87; N, 10.8; Cl, 9.1 %. ES MS *m/z* 290.58 ($[CoL_2]^{2+}$). ^{1}H NMR (CD_3NO_2) δ 11.4 (s, 6H), 17.5 (s, 6H), 19.9 (s, 6H), 28.8 (s, 6H), 46.8 (s, 6H).

Synthesis of [CoL_2][ClO$_4$]$_3$ (3). An acetonitrile solution (15 cm^3) of *L* (300 mg, 1.14 mmol) and Co[ClO$_4$]$_2$·6H$_2$O (209 mg, 0.57 mmol) was stirred in air until all the solid had dissolved. Slow diffusion of diethyl ether vapour into the filtered solution afforded yellow single crystals of the product. Yield 121 mg, 24 %. Found C, 46.5; H, 3.40; N, 9.5; Cl, 12.1 %. Calcd for $C_{34}H_{30}Cl_3CoN_{10}O_{12}$ C, 46.4; H, 3.44; N, 9.6; Cl, 12.1 %. ES MS *m/z* 193.73 ($[CoL_2]^{3+}$). ^{1}H NMR (CD_3NO_2) δ 3.24 (s, 6H, CH_3), 7.40 (d, 6.8 Hz, 6H, Py H^3), 7.45 (pseudo-t, 6.2 Hz, 6H, Py H^5), 8.38 (pseudo-t, 7.3 Hz, 6H, Py H^4), 8.50 (d, 5.9 Hz, 6H, Py H^6). ^{13}C NMR (CD_3NO_2) δ 21.2 (2C, CCH_3), 57.5 (2C, CCH$_3$), 124.8 and 127.2 (both 6C, Py C^3 and C^5), 142.9 (6C, Py C^4), 155.6 (6C, Py C^6), 158.7 (6C, Py C^2).

Synthesis of [PdCl$_2$(*L*)] (4). Addition of [PdCl$_2$(NCMe)$_2$] (148 mg, 0.57 mmol) to a solution of *L* (150 mg, 0.57 mmol) in acetonitrile (20 cm^3) afforded the product as a yellow precipitate, that was collected by filtration and analysed without further purification. Yield 190 mg, 76 %. Found C, 46.45; H, 3.40; N, 9.6; Cl, 16.2 %. Calcd for $C_{17}H_{15}Cl_2N_3Pd$ C, 46.6; H, 3.45; N, 9.6; Cl, 16.2 %. ES MS *m/z* 443.02 ($[PdCl(L)(MeCN)]^+$).

Synthesis of [Ag(*L*)$_2$]NO$_3$ (5a). A mixture of $AgNO_3$ (98 mg, 0.57 mmol) and *L* (150 mg, 0.57 mmol) in MeCN (15 cm^3) rapidly formed a white precipitate. This was sturred for 30 mins, then collected by filtration. Yield 74 mg, 61 %. Found C, 58.6; H, 4.30; N, 14.1 %. Calcd for $C_{34}H_{30}AgN_7O_3$ C, 59.0; H, 4.37; N, 14.2 %. ES MS *m/z* 369.03 ($[AgL]^+$).

Synthesis of [Ag(*L*)$_2$]SbF$_6$ (5b). Method as for **5a**, using $AgSbF_6$ (98 mg, 0.29 mmol). The product was a white solid. Yield 165 mg, 67 %. %. Found C, 47.3; H, 3.50; N, 9.6 %. Calcd for $C_{34}H_{30}AgF_6N_6Sb$ C, 47.1; H, 3.49; N, 9.7 %. ES MS *m/z* 262.13 ($[LH]^+$), 369.03 ($[AgL]^+$). ^{1}H NMR ({CD$_3$}$_2$CO) δ 2.28 (s, 6H, CH_3), 7.29 (pseudo-t, 7.1 Hz, 6H, Py H^5), 7.49 (d, 7.8 Hz, 6H, Py H^3), 7.86 (pseudo-dt, 1.4 and 7.7 Hz, 6H, Py H^4), 8.35 (d, 5.4 Hz, 6H, Py H^6). ^{13}C NMR ({CD$_3$}$_2$CO) δ 28.0 (2C, CCH_3), 59.9 (2C, CCH$_3$), 123.2 and 124.1 (both 6C, Py C^3 and C^5), 138.9 (6C, Py C^4), 150.5 (6C, Py C^6), 164.8 (6C, Py C^2).

Synthesis of [CuI(*L*)] (6). A solution of CuI (145 mg, 0.76 mmol) in MeCN (10 cm^3) was added to a solution of *L* (200 mg, 0.76 mmol) in MeCN (10 cm^3), under an N_2 atmosphere. The reaction stirred at room temperature for two hrs, giving a yellow precipitate that was collected by filtration. Yield 170 mg, 50 %. Found C, 45.2; H, 3.50; N, 8.9 %. Calcd for $C_{17}H_{15}CuIN_3$ C, 45.2; H, 3.35; N, 9.3 %. ES MS *m/z* 450.96 ($[CuI(L)]^+$).

Synthesis of [Cu$_2$I(*L*)$_2$(μ-CO$_3$)]$_2$[CuI$_3$]·2H$_2$O (7a·2H$_2$O). A filtered solution of **6** in MeCN was exposed to air. A green precipitate began to form after a period of few minutes, which was collected and dried *in vacuo*. Found C, 38.9; H, 3.30; N, 8.1 %. Calcd for $C_{70}H_{60}Cu_5I_5N_{12}O_6·2H_2O$ C, 39.0; H, 3.00; N, 7.8 %. Recrystallisation of this material from dmf/Et$_2$O afforded green single crystals of **7b**·4dmf·0.4H$_2$O, in which the iodo ligand in the cation has been partially substituted by hydroxide.

Synthesis of [Cu(CO$_3$)*L*]·4.25H$_2$O (8·4.25H$_2$O) and [CuL_2]I$_2$·8H$_2$O (9·8H$_2$O). A solution of **6** in 1:1 MeCN:H$_2$O was filtered, and left to slowly evaporate under ambient conditions. This afforded two morphologies of crystals. The majority of the crystals were blue prisms of **9**·8H$_2$O, which were sometimes contaminated by a smaller number of darker blue blocks (**8**·4.25H$_2$O). Both compounds were crystallographically analysed, but only **9** was isolated in analytical purity. Found C, 41.5; H, 4.70; N, 8.5 %. Calcd for $C_{34}H_{30}CuI_2N_6·8H_2O$ C, 41.5; H, 4.71; N, 8.5 %. ES MS *m/z* 292.59 ($[CuL_2]^{2+}$), 585.18 ($[CuL_2]^+$).

Single crystal X-ray structure determinations

All diffraction data were collected with an Agilent Supernova dual-source diffractometer using monochromated Cu-K_α (λ = 1.54184 Å) or Mo-K_α radiation (λ = 0.71073 Å). The diffractometer is fitted with an Oxford Cyosystems low-temperature device. Experimental details of structure determinations of each compound at 100 K are given in Table 3. The structures were solved by direct methods (*SHELXS97*[45]), and developed by full least-squares refinement on F^2 (*SHELXL97*[45]). Crystallographic figures were prepared using *X-SEED*,[46] which incorporates *POVRAY*.[47] The MSDA analysis of **9**·8H$_2$O was performed using *PLATON*.[48]

X-ray structure refinements. Unless otherwise stated, all non-H atoms in the structures were refined anisotropically, and C-bound H atoms were placed in calculated positions and refined using a riding model.

No disorder is present in the structure of *L*, and no restraints were applied. H atoms were located in the Fourier map and allowed to refine, with U_{iso} values of 1.2xU_{eq} of the corresponding C atoms for aromatic H atoms, or 1.5xU_{eq}{C} for the methyl group.

The isostructural crystals **1**·4MeCN and **2**·4MeCN have half a formula unit in their asymmetric unit, with Fe(1) or Co(1)

Table 3 Experimental details for the lowest temperature structure determination of each compound in this study. Comparable data at other temperatures, where they were measured, are given in the ESI†.

	L	**1**·4MeCN	**2**·4MeCN	**3**·4MeCN	**3**·H_2O	**4**
Molecular formula	$C_{17}H_{15}N_3$	$C_{42}H_{42}Cl_2FeN_{10}O_8$	$C_{42}H_{42}Cl_2CoN_{10}O_8$	$C_{42}H_{42}Cl_3CoN_{10}O_{12}$	$C_{34}H_{32}Cl_3CoN_6O_{13}$	$C_{17}H_{15}Cl_2N_3Pd$
M_r	261.32	941.61	944.69	1044.14	897.94	438.62
Crystal class	monoclinic	monoclinic	monoclinic	monoclinic	monoclinic	monoclinic
Space group	$P2_1/c$	$P2_1/n$	$P2_1/n$	$P2_1/n$	$P2_1/c$	$P2_1/n$
a (Å)	9.2431(2)	12.0918(10)	12.3122(5)	10.9979(2)	17.1489(4)	9.0049(2)
b (Å)	9.0085(2)	12.7748(8)	12.7314(4)	10.8330(2)	13.8420(3)	18.4245(3)
c (Å)	15.7722(3)	14.8314(11)	14.6894(6)	19.3354(3)	15.2436(3)	10.6172(2)
α (°)	–	–	–	–	–	–
β (°)	95.397(2)	112.518(9)	112.295(5)	92.3450(10)	95.216(2)	112.445(2)
γ (°)	–	–	–	–	–	–
V (Å^3)	1307.47(5)	2116.3(3)	2130.45(14)	2301.70(7)	3603.47(13)	1628.07(5)
Z	4	2	2	2	4	4
μ (mm^{-1})	0.629[a]	0.549[b]	0.594[b]	5.153[a]	0.7764[b]	12.220[a]
T (K)	100(2)	100(2)	100(2)	100(2)	100(2)	100(2)
Measured reflections	5146	11384	10280	8737	35673	5834
Independent reflections	2555	5065	3757	4491	9142	2871
R_{int}	0.023	0.045	0.044	0.022	0.048	0.023
R_1, $I > 2\sigma(I)$[c]	0.036	0.058	0.045	0.031	0.054	0.025
wR_2, all data[d]	0.090	0.153	0.115	0.079	0.146	0.064
Goodness of fit	1.045	1.047	1.053	1.033	1.035	1.107
	5a	**6**·0.5MeCN	**7b**·4dmf·0.4H_2O	**8**·4.25H_2O	**9**·8H_2O	
Molecular formula	$C_{34}H_{30}AgN_7O_3$	$C_{18}H_{16.5}CuIN_{3.5}$	$C_{82}H_{89.92}Cu_5I_{3.88}N_{16}O_{11.52}$	$C_{18}H_{23.5}CuN_3O_{7.25}$	$C_{34}H_{46}CuI_2N_6O_8$	
M_r	692.52	472.29	2294.01	461.44	984.11	
Crystal class	triclinic	monoclinic	monoclinic	monoclinic	monoclinic	
Space group	$P\bar{1}$	$C2/c$	$C2/c$	$P2_1$	$C2/m$	
a (Å)	9.1661(2)	15.7416(2)	38.0784(10)	10.6195(3)	12.9173(8)	
b (Å)	10.4860(3)	12.5216(2)	12.2951(3)	25.6995(7)	13.3786(11)	
c (Å)	16.6632(5)	17.9084(3)	20.3333(5)	14.7591(4)	11.6292(7)	
α (°)	99.769(2)	–	–	–	–	
β (°)	104.448(2)	93.3790(10)	116.027(2)	103.014(3)	103.060(6)	
γ (°)	100.675(2)	–	–	–	–	
V (Å^3)	1484.36(7)	3523.79(9)	8554.2(4)	3924.53(19)	1957.7(2)	
Z	2	8	4	8	2	
μ (mm^{-1})	5.848[a]	15.530[a]	12.932[a]	1.161[b]	2.190[b]	
T (K)	100(2)	100(2)	100(2)	100(2)	120(2)	
Measured reflections	10611	6112	13120	26458	4691	
Independent reflections	5059	3101	7472	13638	2048	
R_{int}	0.031	0.019	0.046	0.041	0.080	
R_1, $I > 2\sigma(I)$[c]	0.024	0.032	0.047	0.041	0.049	
wR_2, all data[d]	0.060	0.078	0.113	0.086	0.120	
Goodness of fit	1.043	1.353	1.018	1.045	1.062	
Flack parameter	–	–	–	–0.006(8)	–	

[a]Collected with Cu-K_α radiation. [b]Collected with Mo-K_α radiation. [c]$R = \Sigma[\,|F_o| - |F_c|\,] / \Sigma|F_o|$ [d]$wR = [\Sigma w(F_o^2 - F_c^2) \;/\; \Sigma wF_o^4]^{1/2}$

lying on the inversion centre 0, ½, ½. One of the unique acetonitrile sites in **1**·4MeCN was modelled over two disorder orientations with a 0.75:0.25 ratio, which share a common wholly occupied nitrile C atom. The fixed restraints C−C = 1.43(2), C−N = 1.16(2) and 1,3-C...N = 2.59(2) Å were applied to that residue. This solvent disorder was not apparent in **2**·4MeCN. All fully occupied non-H atoms in both structures were refined anisotropically.

The crystals of **3**·4MeCN also contain half a formula unit, with Co(1) lying on the inversion centre 0, ½, ½, one whole anion and a half-anion spanning the inversion centre 0, 1, ½. No disorder is present in the model, but the refined restraint Cl−O = 1.44(2) Å was applied to the half-anion to stop the Cl atom migrating to the special position. In contrast, the asymmetric unit of **3**·H_2O contains a complete formula unit, with two unique half-cations on crystallographic inversion centres. One of the three ClO_4^- ions in this structure is disordered over two half-occupied sites, which were refined without restraints. The water H atoms in the hydrate structure were located in the Fourier map and refined, with U_{iso} fixed at 1.5x U_{eq} for the associated O atom.

The asymmetric units of **4**, **5a** and **6**·½MeCN all contain one formula unit; in **6**·½MeCN, the acetonitrile half-molecule spans a crystallographic C_2 axis. No disorder was detected during refinement of any of these structures, and no restraints were applied to them.

There is half a formula unit in the asymmetric unit of **7b**·4dmf·0.4H_2O, comprising one dinuclear complex cation; half a $[CuI_3]^{2-}$ anion lying on a crystallographic C_2 axis; and two dmf molecules. One coordination site of Cu(1) is occupied

by a disordered mixture of iodide [I(1)] and an oxygen ligand [O(1)], which is hydroxide on charge neutrality grounds. The occupancies of these two fragments refined to 0.44 and 0.56 respectively. In addition to two ordered dmf molecules, a weak Fourier peak that is not associated with any other fragment was included in the model as 0.2 equiv of water. This peak is within hydrogen bonding distance of two different carbonato ligands. No restraints were applied to the model during the final least squares cycles. All wholly occupied non-H atoms were refined anisotropically.

The asymmetric unit of **8**·4.25H_2O contains four unique complex molecules and seventeen water molecules No disorder is present in the model, and no restraints were applied. The water H atoms were all located in the Fourier map and allowed to refine, subject to the fixed restraints O−H = 0.90(2) and H...H = 1.47(2) Å, and with U_{iso} equal to 1.5xU_{eq} for the corresponding O atom.

The asymmetric unit of **9**·8H_2O contains one-quarter of a formula unit, with Cu(1) lying on the 2/*m* site ½, ½, 1; atoms C(1)-C(8) lying on the mirror plane *x*, ½, *z*; one half-iodide ion and a half-water molecule lying on the same mirror plane; half a water molecule on the C_2 axis ½, *y*, ½; and a whole water molecule on a general crystallographic site. The water H atoms were located in the Fourier map and allowed to refine, with U_{iso} contrained to 1.5xU_{eq} for the equivalent O atom. The H atoms for the two half-water sites are disordered about those special positions, leading to significant disorder in the hydrogen bonding network.

Other measurements

Elemental microanalyses were performed by the University of Leeds School of Chemistry microanalytical service. Electrospray mass spectra (ESMS) were obtained on a Bruker MicroTOF spectrometer, from MeCN feed solutions. All mass peaks have the correct isotopic distributions for the proposed assignments. Room temperature ^{1}H and ^{13}C NMR spectra were obtained using a Bruker Avance 500 FT spectrometer, operating at 500.1 MHz (^{1}H) or 75 MHz (^{13}C). The variable temperature ^{1}H study was performed on a Bruker DRX500 spectrometer.

Electrochemical measurements were carried out using an Autolab PGSTAT20 voltammetric analyser, under an argon atmosphere in predried CH_3CN containing 0.1 M NBu_4ClO_4 as supporting electrolyte. Voltammetry experiments used a Pt disk working electrode, a Pt rod counterelectrode, and an Ag/AgCl reference electrode. All potentials quoted are referenced to an internal ferrocene/ferrocenium standard, and were obtained at a scan rate of 100 mVs^{-1}.

Magnetic susceptibility measurements were performed on a Quantum Design VSM SQUID magnetometer, in an applied field of 5000 G. A diamagnetic correction for the sample was estimated from Pascal's constants;[49] a diamagnetic correction for the sample holder was also applied to the data.

Acknowledgements

This work was funded by the EPSRC (EP/K012568/1). The authors thank Simon Barrett (University of Leeds) for help with the variable temperature NMR spectra.

Notes and references

School of Chemistry, University of Leeds, Woodhouse Lane, Leeds, UK LS2 9JT. E-mail: a.santoro@leeds.ac.uk and m.a.halcrow@leeds.ac.uk; Fax: +44 113 343 6565; Tel: +44 113 343 6506.

† Electronic Supplementary Information (ESI) available: additional crystallographic Figures and Tables, and cyclic voltammetry data. CCDC 1023797 (*L*), 1023798 (**1**·4MeCN), 1023799 (**2**·4MeCN), 1023800 (**3**·4MeCN), 1023801 (**3**·H_2O), 1023802 (**4**), 1023803 (**5a**), 1023804 (**6**·0.5MeCN), 1023805 (**7b**·4dmf·0.4H_2O), 1023806 (**8**·4.25H_2O) and 1023807 (**9**·8H_2O). For ESI and crystallographic data in CIF or other electronic format see DOI: 10.1039/########.

1 J. P. Wibaut and G. L. C. la Bastide, *Recl. Trav. Chim. Pays-Bas Belg.*, 1933, **52**, 493; F. G. Mann and J. Watson, *J. Org. Chem.*, 1948, **13**, 502; J. P. Wibaut, A. P. de Jonge, H. G. P. van der Voort and P. P. H. L. Otto, *Recl. Trav. Chim. Pays-Bas Belg.*, 1951, **70**, 1054.

2 W. R. McWhinnie, G. C. Kulasingam and J. C. Draper, *J. Chem. Soc. A*, 1966, 1199; G. C. Kulasingam and W. R. McWhinnie, *J. Chem. Soc. A*, 1967, 1253; G. C. Kulasingam and W. R. McWhinnie, *J. Chem. Soc. A*, 1968, 254.

3 R. K. Boggess and D. A. Zatko, *Inorg. Chem.*, 1976, **15**, 626.

4 See *e.g.* K. Kurtev, D. Ribola, R. A. Jones, D. J. Cole-Hamilton and G. Wilkinson, *J. Chem. Soc., Dalton Trans.*, 1980, 55; F. R. Keene, M. R. Snow, P. J. Stephenson and E. R. T. Tiekink, *Inorg. Chem.*, 1988, **27**, 2040; P. K. Byers, A. J. Canty, B. W. Skelton and A. J. White, *Organometallics*, 1990, **9**, 826

5 H. R. Simmonds and D. S. Wright, *Chem. Commun.*, 2012, **48**, 8617.

6 See *e.g.* J. A. Casares, P. Espinet, J. M. Martín-Alvarez and V. Santos, *Inorg. Chem.*, 2006, **45**, 6628; D. Morales, J. Pérez, H. Martinez-García, M. Puerto and I. del Río, *CrystEngComm*, 2011, **13**, 60; M. Bette, T. Kluge, J. Schmidt and D. Steinborn, *Organometallics*, 2013, **32**, 2216.

7 A. Maleckis, J. W. Kampf and M. S. Sanford, *J. Am. Chem. Soc.*, 2013, **135**, 6618.

8 See *e.g.* Y. Hitomi, M. Higuchi, T. Tanaka and T. Funabiki, *J. Mol. Catal. A: Chem.*, 2005, **240**, 207; A. Karam, R. Tenia, M. Martínez, F. López-Linares, C. Albano, A. Diaz-Barrios, Y. Sánchez, E. Catarí, E. Casas, S. Pekerar and A. Albornoz, *J. Mol. Catal. A: Chem.*, 2007, **265**, 127; J. Pérez, D. Morales, L. A. García-Escudero, H. Martinez-García, D. Miguel and P. Bernad, *Dalton Trans.*, 2009, 375; H.-M. Berends, A.-N. Manke, C. Näther, F. Tuczek and P. Kurz, *Dalton Trans.*, 2012, **41**, 6215; S. Maji, L. Vigara, F. Cottone, F. Bozoglian, J. Benet-Buchholz and A. Llobet, *Angew. Chem., Int. Ed.*, 2012, **51**, 5967.

9 See *e.g.* D. V. Griffiths, Y.-K. Cheong, P. Duncanson and M. Motevalli, *Dalton Trans.*, 2011, **40**, 10215; M. A. Gonzalez, M. A. Yim, S. Cheng, A. Moyes, A. J. Hobbs and P. K. Mascharak, *Inorg. Chem.*, 2012, **51**, 601; W. Huber, R. Linder, J. Niesel, U. Schatzschneider, B. Spingler and P. C. Kunz, *Eur. J. Inorg. Chem.*, 2012, 3140.

10 See *e.g.* A. Okazawa, T. Nogami and T. Ishida, *Chem. Phys. Lett.*, 2006, **427**, 333; B. Moubaraki, B. A. Leita, G. J. Halder, S. R. Batten,

P. Jensen, J. P. Smith, J. D. Cashion, C. J. Kepert, J.-F. Létard and K. S. Murray, *Dalton Trans.*, 2007, 4413.

11 P. F. B. Barnard, J. C. Lancaster, M. E. Fernandopulle and W. R. McWhinnie, *J. Chem. Soc., Dalton Trans.*, 1973, 2172.

12 K. R. Adam, P. A. Anderson, T. Astley, I. M. Atkinson, J. M. Charnock, C. D. Garner, J. M. Gulbis, T. W. Hambley, M. A. Hitchman, F. R. Keene and E. R. T. Tiekink, *J. Chem. Soc., Dalton Trans.*, 1997, 519

13 R. Ishikawa, K. Matsumoto, K. Onishi, T. Kubo, A. Fuyuhiro, S. Hayami, K. Inoue, S. Kaizaki and S. Kawata, *Chem. Lett.*, 2009, **38**, 620.

14 N. Hirosawa, Y. Oso, and T. Ishida, *Chem. Lett.*, 2012, **41**, 716.

15 See *e.g.* R. S. Herrick, C. J. Ziegler, D. L. Jameson, C. Aquina, A. Cetin, B. R. Franklin, L. R. Condon, N. Barone and J. Lopez, *Dalton Trans.*, 2008, 3605; J. G. Woollard-Shore, J. P. Holland, M. W. Jones and J. R. Dilworth, *Dalton Trans.*, 2010, **39**, 1576; A. Bakhoda, H. R. Khavasi and N. Safari, *Cryst. Growth Des.*, 2011, **11**, 933; A. Beitat, S. P. Foxon, C.-C. Brombach, H. Hausmann, F. W. Heinemann, F. Hampel, U. Monkowius, C. Hirtenlehner, G. Knör and S. Schindler, *Dalton Trans.*, 2011, **40**, 5090; C. Cui, P. R. Shipman, R. A. Lalancette and F. Jäkle, *Inorg. Chem.*, 2013, **52**, 9440.

16 M. A. Halcrow, *Coord. Chem. Rev.*, 2009, **253**, 2493; L. J. Kershaw Cook, R. Mohammed, G. Sherborne, T. D. Roberts, S. Alvarez and M. A. Halcrow, *Coord. Chem. Rev.*, doi: 10.1016/ j.ccr.2014.08.006.

17 E. A. Ünal, D. Wiedemann, J. Seiffert, J. P. Boyd and A. Grohmann, *Tetrahedron Lett.*, 2012, **53**, 54.

18 G. Dyker and O. Muth, *Eur. J. Org. Chem.*, 2004, 4319; E. A. Ünal, D. Wiedemann, J. Seiffert, J. P. Boyd and A. Grohmann, *Tetrahedron Lett.*, 2012, **53**, 54.

19 See *e.g.* S. Kremer, W. Henke and D. Reinen, *Inorg. Chem.*, 1982, **21**, 3013; C. A. Kilner and M. A. Halcrow, *Dalton Trans.*, 2010, **39**, 9008.

20 P. A. Anderson, T. Astley, M. A. Hitchman, F. R. Keene, B. Moubaraki, K. S. Murray, B. W. Skelton, E. R. T. Tiekink, H. Toftlund and A. H. White, *J. Chem. Soc*., *Dalton Trans*., 2000, 3505.

21 E. S. Kucharski W. R. McWhinnie and A. H. White, *Aust. J. Chem.*, 1978, **31**, 53; C. S. Alvarez, F. García, S. M. Humphrey, A. D. Hopkins, R. A. Kowenicki, M. McPartlin, R. A. Layfield, R. Raja, M. C. Rogers, A. D. Woods and D. S. Wright, *Chem. Commun.*, 2005, 198 ; A. Bakhoda, H. R. Khavasi and N. Safari, *Cryst. Growth Des.*, 2011, **11**, 933.

22 E. S. Kucharski W. R. McWhinnie and A. H. White, *Aust. J. Chem.*, 1978, **31**, 2647; B. A. Trofimov, N. K. Gurasova, A. V. Artem'ev, S. F. Malysheva, N. A. Belogorlova, A. O. Korocheva, O. N. Kazheva, G. G. Alexandrov and O. A. Dyachenko, *Mendeleev Commun.*, 2012, **22**, 187; Y. Tsunezumi, K. Matsumoto, S. Hayami, A. Fuyuhiro and S. Kawata, *Acta Cryst. Sect. E*, 2014, **70**, m96.

23 R. K. Boggess, J. W. Hughes, C. W. Chew and J. J. Kemper, *J. Inorg. Nucl. Chem.*, 1981, **43**, 939.

24 T. A. Hafeli and F. R. Keene, *Aust. J. Chem.*, 1988, **41**, 1379.

25 A. G. Young and L. R. Hanton, *Coord. Chem. Rev.*, 2008, **252**, 1346.

26 Although it suffers from twinning, a preliminary structure solution of **5b** also demonstrated the presence of square planar $[AgL_2]^+$ centres. Unit cell data $C_{34}H_{30}AgF_6N_6Sb$, M_r = 866.24, orthorhombic, a = 32.1182(12), b = 22.3288(9), c = 18.1232(7) Å.

27 A. J. Canty, N. J. Minchin, L. M. Engelhardt, B. W. Skelton and A. H. White, *J. Chem. Soc., Dalton Trans.*, 1986, 645.

28 J. Burgess and P. J. Steel, *Coord. Chem. Rev.*, 2011, **255**, 2094.

29 N. E. Brese and M. O'Keeffe, *Acta Cryst., Sect. B*, 1991, **47**, 192.

30 D. L. Reger, J. R. Gardinier and M. D. Smith, *Polyhedron*, 2004, **23**, 291; K. Matsumoto, M. Kannami and M. Oda, *Chem. Lett.*, 2004, **33**, 1096.

31 See *e.g.* R. A. Walton and R. W. Matthews, *Inorg. Chem.*, 1971, **10**, 1433; W. R. Scheidt, J. U. Mondal, C. W. Eigenbrot, A. Adler, L. J. Radonovich and J. L. Hoard, *Inorg. Chem.*, 1986, **25**, 795; J. L. Shaw, J. Wolowska, D. Collison, J. A. K. Howard, E. J. L. McInnes, J. McMaster, A. J. Blake, C. Wilson and M. Schröder, *J. Am. Chem. Soc.*, 2006, **128**, 13827; S. Kandaiah, E.-M. Peters and M. Jansen, *Z. Anorg. Allg. Chem.*, 2008, **634**, 2483; S. Kandaiah, R. Huebner and M. Jansen, *Polyhedron*, 2012, **48**, 68.

32 N. J. English, M. M. El-Hendawy, D. A. Mooney and J. M. D. MacElroy, *Coord. Chem. Rev.*, 2014, **269**, 85.

33 M. R. Churchill, G. Davies, M. A. El-Sayed, M. F. El-Shazly, J. P. Hutchinson and M. W. Rupich, *Inorg. Chem.*, 1980, **19**, 201.

34 R. R. Gagne, R. S. Gall, G. C. Lisensky, R. E. Marsh and L. M. Speltz, *Inorg. Chem.*, 1979, **18**, 771; A. R. Davis and F. W. B. Einstein, *Inorg. Chem.*, 1980, **19**, 1203; N. Kitajima, T. Koda, S. Hashimoto, T. Kitagawa and Y. Moro-oka, *J. Am. Chem. Soc.*, 1991, **113**, 5664; A. L. van den Brenk, K. A. Byriel, D. P. Fairlie, L. R. Gahan, G. R. Hanson, C. J. Hawkins, A. Jones, C. H. L. Kennard, B. Moubaraki and K. S. Murray, *Inorg. Chem.*, 1994, **33**, 3549.

35 J. L. Schneider, V. G. Young jr. and W. B. Tolman, *Iorg. Chem.*, 1996, **35**, 5410; A. Escuer, F. A. Mautner, E. Peñalba and R. Vicente, *Inorg. Chem.*, 1998, **37**, 4190; B. Verdejo, J. Aguilar, E. García-España, P. Gaviña, J. Latorre, C. Soriano, J. M. Llinares and A. Doménech, *Inorg. Chem.*, 2006, **45**, 3803.

36 P. V. Bernhardt, *Inorg. Chem.*, 2001, **40**, 1086; A. Company, J.-E. Jee, X. Ribas, J. M. Lopez-Valbuena, L. Gómez, M. Corbella, A. Llobet, J. Mahía, J. Benet-Buchholz, M. Costas and R. van Eldik, *Inorg. Chem.*, 2007, **46**, 9098; I. Vera, L. Dominguez, J. Ellena and M. H. Torre, *Z. Naturforsch., Teil B,* 2008, **63**, 548; R. A. Joy, H. Arman, S. Xiang and G. T. Musie, *Inorg. Chim. Acta* 2013, **394**, 220.

37 See *e.g.* N. Ehlers and R. Mattes, *Inorg. Chim. Acta*, 1995, **236**, 203; B. Breener and P. H. Walton, *J. Chem. Soc., Dalton Trans.*, 1997, 3733; C. Bergquist, T. Fillebeen, M. M. Morlock and G. Parkin, *J. Am. Chem. Sco.*, 2003, **115**, 6189; U. P. Singh, P. Babbar, P. Tyagi and T. Weyhermuller, *Transition Met. Chem.*, 2008, **33**, 931 ; W. Sattler and G. Parkin, *Chem. Sci.*, 2012, **3**, 2015; C. T. Saouma, C. C. Lu, M. W. Day and J. C. Peters, *Chem. Sci.*, 2013, **4**, 4042; B. J. Truscott, D. J. Nelson, A. M. Z. Slawin and S. P. Nolan, *Chem. Commun.*, 2014, **50**, 286.

38 A. W. Addison, T. N. Rao, J. Reedijk, J. van Rijn and G. C. Verschoor, *J. Chem. Soc., Dalton Trans.*, 1984 1349. An ideal square pyramidal coordination geometry is characterised by $\tau = 0$, while an ideal trigonal pyramid yields $\tau = 1$.

39 L. Infantes and S. Motherwell, *CrystEngComm*, 2002, **4**, 454; L. Infantes, J. Chisholm and S. Motherwell, *CrystEngComm*, 2003, **5**, 480.

40 J. D. Dunitz, V. Schomaker and K. N. Trueblood, *J. Phys. Chem.*, 1988, **92**, 856.

41 L. R. Falvello, *J. Chem. Soc., Dalton Trans.*, 1997, 4463.

42 M. A. Halcrow, *Dalton Trans.*, 2003, 4375; M. A. Halcrow, *Chem. Soc. Rev.*, 2013, **42**, 1784.
43 T. Astley, P. J. Ellis, H. C. Freeman, M. A. Hitchman, F. R. Keene and E. R. T. Tiekink, *J. Chem. Soc., Dalton Trans.*, 1995, 595; T. Astley, H. Headlam, M. A. Hitchman, F. R. Keene, J. Pilbrow, H. Stratemeier, E. R. T. Tiekink and Y. C. Zhong, *J. Chem. Soc., Dalton Trans.*, 1995, 3809.
44 I. Abrunhosa, L. Delain-Bioton, A.-C. Gaumont, M. Gulea and S. Masson, *Tetrahedron*, 2004, **60**, 9263.
45 G. M. Sheldrick, *Acta Crystallogr., Sect. A*, 2008, **64**, 112
46 L. J. Barbour, *J. Supramol. Chem.*, 2001, **1**, 189.
47 *POVRAY*, v. 3.5, Persistence of Vision Raytracer Pty. Ltd., Williamstown, Victoria, Australia, 2002. http://www.povray.org.
48 A. L. Spek, *J. Appl. Cryst.*, 2003, **36**, 7.
49 C. J. O'Connor, *Prog. Inorg. Chem.*, 1982, **29**, 203.